

Real-Time Implementation of Reduced Order Compensators on a Cantilever Beam

Brian M. Lewis, and Hien T. Tran, *Member, SIAM*

Abstract—In this paper, we consider the real-time synthesis of reduced order model based control methodologies for the attenuation of vibrations of a cantilever beam caused by either a transient spike disturbance or a narrow-band exogenous force in a smart structure paradigm. By a narrow-band exogenous force we mean a periodic force over a narrow frequency band or a particular harmonic. The control methods under consideration are based on the minimization of two specific quadratic cost functionals. One of these cost functionals is a typical time domain cost functional constrained by an affine plant. The other is a cost functional that is frequency dependent. These control methods have been used successfully in various applications but this investigation differs from other works in that it emphasizes the development of real-time control methodologies based on reduced order models derived from physical first principles. In particular, we consider two reduced order model based control approaches: reduce the order of the model followed by control formulation and formulate a control based on the full order model followed by control reduction.

Index Terms—cantilever beam, frequency shaping, real-time, balanced realization, LQG balancing.

I. INTRODUCTION

EVEN with advances in technology today, mathematical models derived from physical first principles are still too complex for implementation in real-time. To overcome this complexity, a number of techniques have been proposed to either reduce the order of the model and then formulate a control (reduce then synthesize) ([1], [2], [3], [4], [5], [6]) or to formulate a control based on the full order model and then reduce the control directly (synthesize then reduce) ([7], [8], [9]). There are a number of differing opinions as to which of these methodologies contains more information about the underlying dynamics of the system (usually modeled by a system of partial differential equations (PDE)). However, here we don't address this issue nor do we rigorously present theoretical aspects associated with the reduced order methods. Instead, we give a computational overview of how to implement the reduced order methods and discuss real-time implementation details and dilemmas that we have encountered, some of which, to our knowledge, have not been addressed. The structure on which we have implemented the reduced order compensators is an Euler-Bernoulli beam with piezoceramic (PZT) actuators/sensors.

We have implemented two reduced order compensators. We first discuss one of the classic reduce then synthesize methods, balanced realization and truncation (otherwise

known as open loop balancing) [10]. We then discuss a synthesize then reduce method, LQG balancing (sometimes referred to as closed loop balancing in the literature) ([11], [12]). It should be emphasized that it is not our intent to do a head to head competition of these approaches, we believe they all have strengths and weaknesses and their use in real-time should be situationally dependent. It is our intent to show that each method can be used in real-time and explain in a precise way how each can be implemented and some of the complexities involved with their implementation. We have successfully implemented reduced order controllers with dimensions ranging from 4 to 10 (in even multiples) for each technique. However, for the sake of brevity we present the lowest order control that achieved damping of the vibration at a level indistinguishable (by eye) from the next higher order model.

II. THE EULER-BERNOULLI BEAM MODEL

In this section we briefly describe the partial differential equation (PDE) used to model the cantilever beam and an approximation to this PDE that is feasible for real-time compensation. To this end we consider a flat rectangular cantilevered beam, satisfying the Euler-Bernoulli (EB) displacement and Kelvin-Voigt (KV) damping hypotheses, to which piezoelectric patch actuators/sensors are mounted in a symmetric and opposing manner. Figure 1 is an illustration of this beam from the side. As depicted, we impose a coordinate system with x -direction along the length of the beam and y -direction along the direction of transverse displacement. The end located at $x = 0$ is clamped while the end located at $x = \ell$ is free. As depicted in the figure, the beam has dimensions: length ℓ , width h , and thickness T_b . The patches are located between the points x_1 and x_2 and have a thickness of T_p (not labelled in the figure). Further, the patches have the same width, h , as the beam. As is necessary for the EB hypotheses, the beam has a constant cross section and is much smaller across than the length of the beam so that only small transverse displacement occurs and there is no torsion or twisting. The transverse displacements $y(t, x)$ of the beam, subjected only to forces and moments due to the patches and viscous air damping, are given by (see [13])

$$\rho(x) \frac{\partial^2 y}{\partial t^2} + \gamma \frac{\partial y}{\partial t} + \frac{\partial^2 M}{\partial x^2} + \frac{\partial^2 M_p}{\partial x^2} = 0. \quad (1)$$

The linear mass density, $\rho(x)$, is piecewise constant due to the contribution of the patches and is given by

$$\rho(x) = \rho_b T_b h + 2\rho_p T_p h \chi_{[x_1, x_2]}(x),$$

where χ denotes the characteristic function given by

$$\chi_{[x_1, x_2]}(x) = \begin{cases} 1 & \text{if } x \in [x_1, x_2] \\ 0 & \text{otherwise} \end{cases},$$

Manuscript received October 11, 2010; revised January 07, 2011. This work was carried out while B.M. Lewis was with the Department of Mathematics and the Center for Research in Scientific Computation, North Carolina State University, Raleigh, NC, 27695.

B.M. Lewis is with the MIT Lincoln Laboratory, 244 Wood Street, Lexington, MA, 02420 USA e-mail: blewis@ll.mit.edu.

H.T. Tran is with the Department of Mathematics and the Center for Research in Scientific Computation, North Carolina State University, Raleigh, NC, 27695 USA e-mail: tran@math.ncsu.edu.

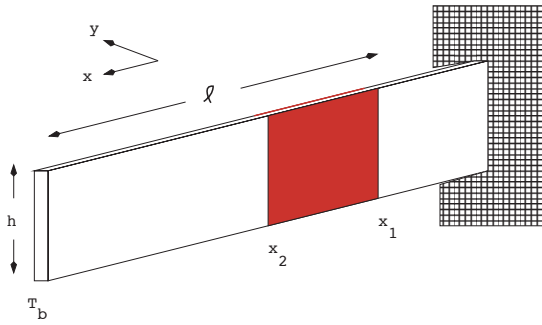


Fig. 1. A cantilever beam with piezoelectric patches

and ρ_b and ρ_p are the volumetric mass density of the beam and patches, respectively. We denote the viscous air damping parameter by γ so that the second term of (1), which is proportional to the transverse velocity, represents the air damping term. The internal moment is given by

$$M(t, x) = EI(x) \frac{\partial^2 y}{\partial x^2}(t, x) + c_D I(x) \frac{\partial^3 y}{\partial x^2 \partial t}(t, x), \quad (2)$$

where $EI(x)$ is the Young's modulus multiplied by the moment of inertia and $c_D I(x)$ is the Kelvin-Voigt damping multiplied by the moment of inertia, both of which are piecewise constant due to the patches. These functions are given by

$$EI(x) = E_b \frac{T_b^3 h}{12} + \frac{2h}{3} E_p a_3 \chi_{[x_1, x_2]}(x) \quad (3)$$

and

$$c_D I(x) = c_{D_b} \frac{T_b^3 h}{12} + \frac{2h}{3} c_{D_p} a_3 \chi_{[x_1, x_2]}(x), \quad (4)$$

where $a_3 = (T_b/2 + T_p)^3 - T_b^3/8$ and the subscripts b and p represent the beam patch parameters. Finally, we have that the moment due to the patch is given by

$$M_p(t, x) = -\mathcal{K} \chi_{[x_1, x_2]}(x) (V_1(t) - V_2(t)), \quad (5)$$

where $\mathcal{K} = -\frac{1}{2} E_p h d_{31} (T_b + T_p)$ and d_{31} is the piezoelectric strain parameter while V_1 and V_2 represent the voltages applied to the front and back piezoelectric patches, respectively.

The cantilever beam has two boundary conditions at each end and initial conditions for both the displacement and velocity. At the fixed end, $x = 0$, the associated boundary conditions on the transverse displacement are

$$y(t, 0) = \frac{\partial y}{\partial x}(t, 0) = 0. \quad (6)$$

At the free end of the beam, $x = \ell$, the boundary conditions allow for free moment and shearing force and are given by

$$M(t, \ell) = \frac{\partial}{\partial x} M(t, \ell) = 0. \quad (7)$$

The initial conditions on the displacement and velocity are

$$y(0, x) = y_0(x), \quad \frac{\partial y}{\partial t}(0, x) = y_1(x). \quad (8)$$

For a detailed derivation of the beam model we refer the interested reader to [13]. For real-time implementation we employed the Galerkin approximation using modified cubic spline functions that conform to the boundary conditions at the clamped end, $x = 0$ ([14], [15], [16]). The beam and patch parameters were identified from experimental data using an inverse least-squares formulation [14]. Their estimated and measured values can be found in [15], [16].

III. EXPERIMENTAL SETUP AND CONTROL METHODOLOGY

In this section we summarize the real-time experimental set-up and the control methodologies for the attenuation of beam vibrations. Since the control that we are going to present is to be implemented in real-time, we must first describe the scenario of the test bed. The cantilever beam is depicted in Figure 1. The periodic disturbance is created using the front patch. This ACX (model QP10N) patch allows a maximum of 200 volts and is approximately 0.0508 m in length and 0.0254 m in height. The physical dimensions of the patch were used in the model formulation. The Simulink (The MathWorks, Inc.) generated disturbance (with 0.5 volt amplitude) is passed through the digital to analog converter (a DSP controller subsystem of the *dSpace* DS1103 PowerPC Controller Board with 36 ADC channels and 8 DAC channels) resulting in a 5 volt signal and then through a low pass filter (Frequency Devices Model 9002) to remove any noise created during D/A conversion. The signal is then amplified (Krohn-Hite Model 7600 wideband amplifier) by 28 dB so that the resultant sinusoidal disturbance level, which is approximately 125.6 volt, submitted to the patch was appropriate. The process of creating the disturbance is depicted in Figure 2 starting with the "source" box and ending at the patch.

The control is based on feedback so we must detail the method to which we obtain beam data. We use a Bentley Nevada proximity probe that is located at $\hat{x} = 0.13$ m (see Figure 2). The location of the sensing device was not optimized. However, it was chosen to avoid the node location for the first four modes. In addition, since the disturbance frequency was chosen so as to not excite the beam at a fundamental frequency, the beam disturbance was observable. We are able, then, to collect displacement data with minimal alterations to our composite structure. There is one slight alteration - a small metal square that is 0.01 mm in depth. Since this metal square is very thin, its effects on the dynamics of the beam were neglected and, therefore, were not modeled. Using the *dSpace Prototyper*, we are able to convert this analog feedback data to a digital signal. In Figure 3 we present a photograph of the beam used for the experimentation at the laboratory (the proximity probe is also displayed in this picture).

Two kinds of disturbance were investigated. The first disturbance that we considered is that of an approximate delta function that we estimate with a triangular voltage spike with a duration of 0.01 seconds and a magnitude of 125.6 volts. This disturbance is important as it allows for an implementation of LQG balancing as it is intended, a direct reduction on the controller. For this disturbance, the feedback control that was implemented is the classical linear quadratic regulation (LQR) control [14]. The second disturbance is periodic with a frequency of 50 Hz. To mitigate this persistent disturbance, we employed a feedback control methodology based on the frequency shaping technique ([16], [17]). Both control laws were developed assuming full knowledge of the state as well as full knowledge of the disturbance. However, often (and especially in the test bed) the full knowledge of the state is not feasible. Hence, in order to compensate the system we need an estimator to take the

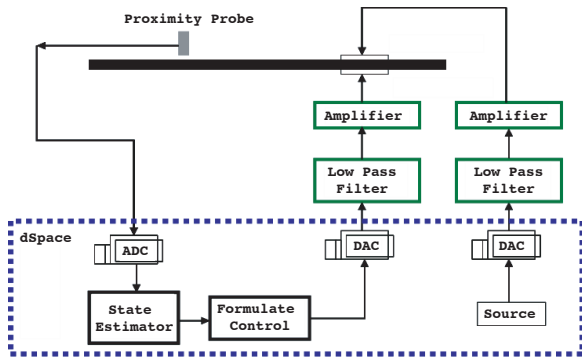


Fig. 2. Flow chart for the real-time control of the cantilever beam

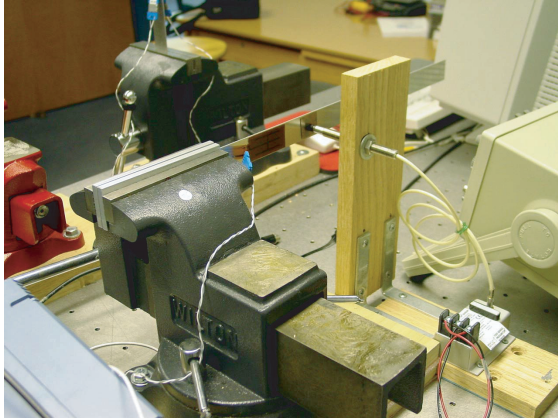


Fig. 3. A photograph of the actual experiment

one displacement value at each time step and instantaneously estimate the states for the beam at the nodal points. For the transient disturbance this estimator is based on the dual LQR equation but for the periodic disturbance we must use an augmented system to estimate the persistent disturbance. We note that the compensated control is also converted, filtered, and then amplified by 28 dB so that it must be scaled. This entire process is depicted in Figure 2 starting with the proximity probe and ending with the control being sent to the patch. The implementation is carried out using Simulink and *dSpace*'s Total Development Environment (TDE), a state-of-the-art software tool for the whole development process, from control design through implementation to verification.

IV. BALANCED REALIZATION AND TRUNCATION

Consider the following finite-dimensional controlled system:

$$\begin{aligned}\dot{x} &= Ax + Bu \\ y &= Cx,\end{aligned}$$

where $x \in R^n$, $u \in R^m$, $y \in R^p$, A , B , and C are matrices of appropriate dimensions. Balanced realization (also called open-loop balancing) is one of the classical techniques for finding a reduced order system. Essentially the technique seeks to retain the states that are easiest to observe and control. The information regarding the controllability and observability of the states can be inferred in part from the controllability and observability grammians, which are given by

$$W_c(t) = \int_0^t e^{At} B B^T e^{A^T t} dt \quad (9)$$

and

$$W_o(t) = \int_0^t e^{A^T t} C^T C e^{At} dt, \quad (10)$$

respectively. The corresponding differential forms are

$$\dot{W}_c = A W_c + W_c A^T + B B^T \quad (11)$$

and

$$\dot{W}_o = A^T W_o + W_o A + C^T C. \quad (12)$$

If the system is stable, the time derivatives on the left of both (11) and (12) are zero. Hence, the grammians to be solved for the stationary stable problem are

$$A W_c + W_c A^T = -B B^T \quad (13)$$

and

$$A^T W_o + W_o A = -C^T C. \quad (14)$$

Information about the reachable and observable states of the system can be extracted using W_c and W_o . Consider a transformation of the form $\tilde{x} = P x$. The new system dynamics have the form

$$\dot{\tilde{x}} = P A P^{-1} \tilde{x} + P B u$$

with output given by

$$\tilde{y} = C P^{-1} \tilde{x}.$$

For the transformed system, the steady state Lyapunov equations become

$$P A P^{-1} \tilde{W}_c + \tilde{W}_c P^{-T} A^T P^T = -P B B^T P^T \quad (15)$$

and

$$P^{-T} A^T P^T \tilde{W}_o + \tilde{W}_o P A P^{-1} = -P^{-T} C^T C P^{-1}. \quad (16)$$

Hence, if the transformation is to inherit the stability of the original system, the solutions to the transformed Lyapunov equations must be

$$\tilde{W}_c = P W_c P^T \quad \text{and} \quad \tilde{W}_o = P^{-T} W_o P^{-1}.$$

Since W_c and W_o can be used to obtain information about the reachable and observable states, respectively, it can be seen that these transformations indicate that the eigenvalue information is dependent upon the realization. However, the grammian product is invariant under the transformation as evidenced by

$$\lambda(\tilde{W}_c \tilde{W}_o) = \lambda(P W_c P^T P^{-T} W_o P^{-1}) = \lambda(W_c W_o).$$

These eigenvalues are referred to as Hankel singular values. The above observations suggest the following algorithm to balance the system:

Algorithm 4.1: Balanced Realization

- 1) Compute W_c and W_o .
- 2) Find L_c and L_o such that $W_c = L_c L_c^T$ and $W_o = L_o L_o^T$ using either the singular value decomposition or Cholesky decomposition.
- 3) Compute the singular value decomposition of $L_o^T L_c = \mathcal{U} \Sigma \mathcal{V}^T$.
- 4) The balancing transform is given by

$$P = \Sigma^{-1/2} \mathcal{U}^T L_o^T$$

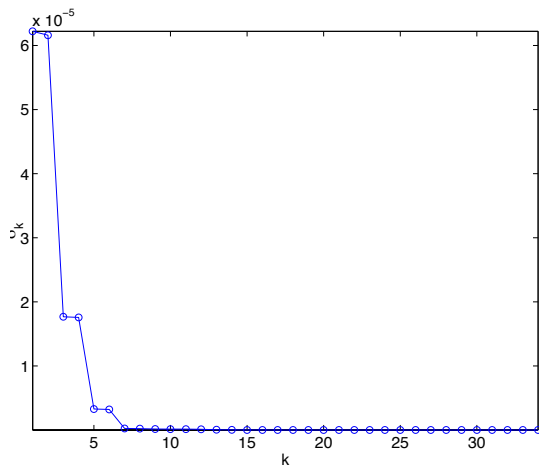


Fig. 4. Hankel singular values as a function of dimension k

and, to avoid numerical difficulties, we compute P^{-1} from the formula

$$P^{-1} = L_c \mathcal{V} \Sigma^{-1/2}.$$

The beauty of this balanced realization is that

$$PW_c P^T = \Sigma^{-1/2} \mathcal{U}^T L_o^T L_c L_c^T L_o \mathcal{U} \Sigma^{-1/2} = \Sigma$$

and

$$P^{-T} W_o P^{-1} = \Sigma^{-1/2} \mathcal{V}^T L_c^T L_o L_o^T L_c \mathcal{V} \Sigma^{-1/2} = \Sigma.$$

We note that in many cases in which the system is controllable and observable the standard MATLAB function *lyap.m* returns a solution to the Lyapunov equation that is not positive definite (which of course does not have a Cholesky decomposition). However, by using routines that solve the Lyapunov equation for the Cholesky decomposition of the solution, (e.g. solve for the lower triangular L_c in

$$A L_c L_c^T + L_c L_c^T A^T = -B B^T,$$

instead of W_c in (13)) we can avoid this situation. Tested routines are in existence in packages such as SLICOT that are freely available [18].

With the balancing transformations it is then possible to reduce the order of the system. Once a reduction size has been decided upon we can partition the balanced system matrices as

$$\dot{\tilde{x}} = L P A P^{-1} L^T \tilde{x} + L P B u \quad (17)$$

and

$$\tilde{y} = C P^{-1} L^T \tilde{x}, \quad (18)$$

where $L = [I_{r \times r} \ 0]$. From which we can use the frequency shaping method of Section III to formulate the controller for the periodic disturbance compensator.

An indication of the amount one can reduce is the Hankel singular values given by $\sigma_i = \sqrt{\lambda_i(W_c W_o)}$. In Figure 4 we present a depiction of first several ordered eigenvalues. We notice that there are several sharp declines in the value of the eigenvalues. However, this plot does not provide a definitive reduction order (it could easily be 2, 4, 6, or 10). For a persistent disturbance of 50 Hz sinusoid, we display the results for $n_r = 10$ in Figures 5. It is noted that the original finite-dimensional system is of order $n = 34$ (17 displacement and

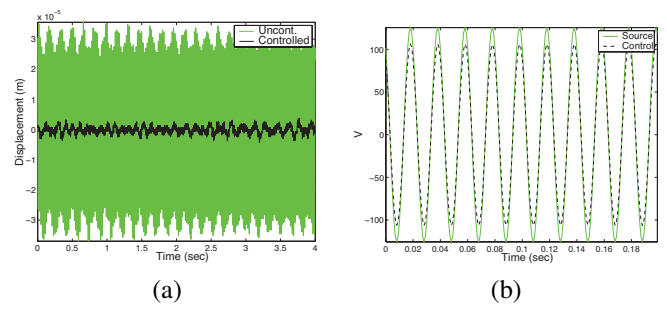


Fig. 5. Balanced realization results, (a) real-time periodic controlled dynamics versus uncontrolled (Uncont.) dynamics ($n_r = 10$) and (b) real-time frequency shaping control voltage

17 velocities from the Galerkin approximation using 17 cubic splines). Hence, we achieve a reduction in dimension from 34 to 10, which is quite sufficient in this control scenario. Figure 5 (a) depicts the uncontrolled periodic model response of the full order model (of dimension 34) with the open loop balanced reduced model (of order $n_r = 10$). The control voltage that is applied to the patch is depicted in Figure 5 (b).

V. LQG BALANCING AND TRUNCATION

It has been theorized that reduced order controllers formulated from reduced order models lose much of the physics of the PDE system [19]. Thus, it is of interest to capture the physics of the system in the control (by formulating the control using the full order model) and then to reduce the controller directly. Here, we take cues from the balanced realization and truncation technique. However, we also assume that we already have knowledge of the Riccati solutions. Hence, this technique is often referred to as closed loop balancing. That is, for the controlled system

$$\dot{x} = Ax + Bu$$

with output modeled by

$$y = Cx$$

the estimator has the form

$$\dot{x}_e = Ax_e + Bu + L(y - Cx_e).$$

Using LQG techniques, the feedback controller is given by

$$u = -Kx, \text{ where } K = R^{-1} B^T \Pi,$$

and Π solves the constant algebraic Riccati equation

$$\Pi A + A^T \Pi - \Pi B R^{-1} B^T \Pi + Q = 0.$$

Likewise, the estimator gain matrix $L = \Gamma C^T V^{-1}$, where Γ solves the dual algebraic Riccati equation given by

$$\Gamma A^T + A \Gamma - \Gamma C^T V^{-1} C \Gamma + U = 0.$$

Often in the literature for LQG balancing R and V are set to unity and Q and U are set to $C^T C$ and $B B^T$, respectively. However, we leave these matrices generalized for the time being (with the assumptions of Q and U being symmetric, positive semi-definite and R and V being symmetric, positive definite). Under the transformation $\tilde{x} = Px$ we have that the transformed system dynamics are given by

$$\dot{\tilde{x}} = P A P^{-1} \tilde{x} + P B u$$

with output given by

$$y = CP^{-1}\tilde{x}.$$

The estimator for the transformed system is

$$\dot{\tilde{x}}_e = PAP^{-1}x_e + PBu + PL(y - CP^{-1}x_e).$$

Using methods similar to those given in the previous section we find that the solutions $\tilde{\Pi}$ and $\tilde{\Gamma}$ to the transformed Riccati equations

$$\tilde{\Pi}PAP^{-1} + (PAP^{-1})^T\tilde{\Pi} - \tilde{\Pi}PBR^{-1}(PB)^T\tilde{\Pi} + \tilde{Q} = 0$$

and

$$\tilde{\Gamma}(PAP^{-1})^T + PAP^{-1}\tilde{\Gamma} - \tilde{\Gamma}(CP^{-1})^TV^{-1}CP^{-1}\tilde{\Gamma} + \tilde{U} = 0$$

are given by

$$\tilde{\Pi} = P^{-T}\Pi P^{-1} \text{ and } \tilde{\Gamma} = P\Gamma P^T,$$

where

$$\tilde{Q} = P^{-T}\Pi P^{-1} \text{ and } \tilde{U} = PUP^T.$$

As above, the Riccati product is invariant under the transformation as evidenced by

$$\lambda(\tilde{\Pi}\tilde{\Gamma}) = \lambda(P^{-T}\Pi P^{-1}P\Gamma P^T) = \lambda(\Pi\Gamma).$$

These eigenvalues are referred to as Riccati singular values by some [19] and LQG singular values by others [20]. We wish to again use a transformation matrix P that will diagonalize $\tilde{\Pi}$ and $\tilde{\Gamma}$. Following a methodology similar to open loop balancing, our approach is given in the following algorithm:

Algorithm 5.1: LQG Balancing

- 1) Compute Π and Γ .
- 2) Find S and R such that $\Pi = SS^T$ and $\Gamma = \mathcal{R}\mathcal{R}^T$ using either the singular value decomposition or Cholesky decomposition.
- 3) Compute the singular value decomposition of $S^T\mathcal{R} = \mathcal{U}\Sigma\mathcal{V}^T$.
- 4) The balancing transform is given by

$$P = \Sigma^{-1/2}\mathcal{U}^T S^T$$

and, to avoid numerical difficulties, we employ the following formula to compute P^{-1}

$$P^{-1} = \mathcal{R}\mathcal{V}\Sigma^{-1/2}.$$

We see that this transformation has the property that

$$P\Gamma P^T = \Sigma^{-1/2}\mathcal{U}^T S^T \mathcal{R}\mathcal{R}^T S \Sigma^{-1/2} = \Sigma$$

and

$$P^{-T}\Pi P^{-1} = \Sigma^{-1/2}\mathcal{V}^T \mathcal{R}^T S S^T \mathcal{R}\mathcal{V}\Sigma^{-1/2} = \Sigma.$$

We now face some new and interesting dilemmas in implementation that have not yet been discussed to our knowledge. The tuning for this reduced order method, in it's intended form, is quite difficult. We mention the intended form of LQG balancing because all of the literature uses the method as a controller reduction. Hence we design the controller using the full order system, reduce the controller and system simultaneously and use the transformed controller directly. This poses some difficulty as we do not only have to find parameters that result in an efficient control but also so that the

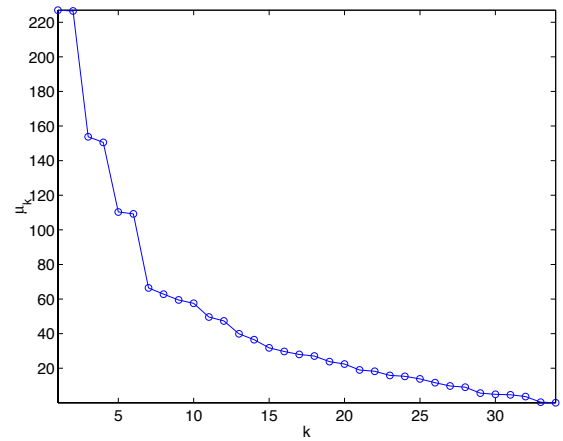


Fig. 6. Singular values of the Riccati operator

reduced order model is accurate. Since the periodic control that we have presented has augmented matrices of different dimensions for the observer and controller we see that LQG controller reduction does not apply directly (however, we will show that using the closed loop balancing results in an accurate model so that we can use the reduced order model to synthesize a periodic control). Hence, the results we present for LQG balancing in the spirit of controller reduction only pertain to the transient delta spike control. As mentioned, it is common in LQG balancing to set $R = V = 1$, $Q = C^T C$, and $U = BB^T$. We first attempt to reduce the dimension of the system and controller using these gain matrices for the algorithm. We again consider the associated singular values, in the case the Riccati singular values. In Figure 6 we display the Riccati singular values. However, we see that, as in balanced realization and truncation, there are a number of possible reduction points (usually of even increment). Hence, we again attempt to reduce at $n_r = 4, 6, 8, 10$. Figure 7 (a) is the open loop response of the full order and reduced order system (with $n_r = 4$). Notice that the reduced order model very closely resembles the full order model. However, in Figure 7 (b) we present the simulated closed loop impulse response (the model with system matrix $A - BK$) and we see that in the full and reduced order case the dynamics are relatively unchanged. We made an attempt to use the control in real-time and we see in Figure 7 (c) that the control has very little influence on the dynamics (perhaps they are even worse). Since it doesn't work in the full order case we cannot expect it to work upon reduction. Hence, with this formulation we do not have enough (pardon the pun) control over the control. For the next try at LQG balancing we choose the weighting matrices so that a stabilizing control is obtained with the full order model. However, we observe that in this case the reduced order model based control dynamics are not close to the full order system. This suggests that we must tune the parameters with both open loop and closed loop responses in mind. We found sufficient parameters (for $n_r = 10$) to be $q = 5 \times 10^2$, $r = 5 \times 10^{-4}$, $u = 0.1$, and $v = 5 \times 10^{-3}$. The results for this scenario are given in Figure 8. The control gains are formulated with direct transformations of the solutions to the full order Riccati equations.

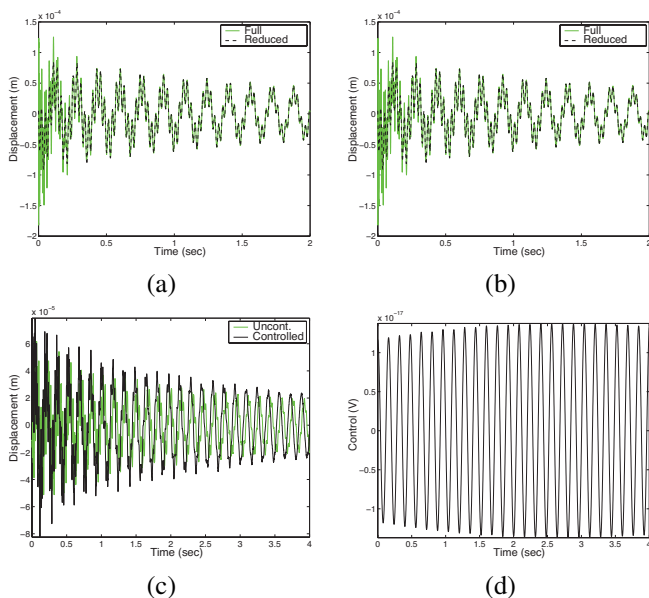


Fig. 7. LQG Balancing with $R = V = 1$, $Q = C^T C$, and $U = B B^T$, (a) impulse response ($n_r = 4$), (b) closed loop impulse response ($\dot{x} = (A - BK)x + \delta(0)$) ($n_r = 10$), (c) real-time transient controlled dynamics versus uncontrolled (Uncont.) dynamics ($n_r = 4$), and (d) real-time LQR control voltage

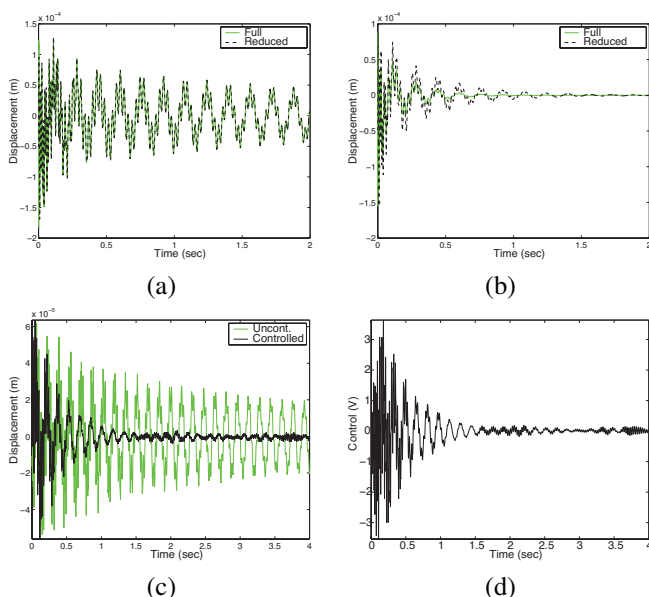


Fig. 8. LQG Balancing, (a) impulse response ($n_r = 10$), (b) closed loop impulse response ($\dot{x} = (A - BK)x + \delta(0)$) ($n_r = 10$), (c) real-time transient controlled dynamics versus uncontrolled (Uncont.) dynamics ($n_r = 10$), and (d) real-time LQR control voltage

Thus with this example we see that, to use LQG balancing for controller reduction, it is not enough for the reduced order model to be precise or for the full order control to work well. We need a balance of both.

VI. CONCLUSION

In this paper, we presented successful real-time implementation of two reduced order models based feedback control methodologies. In particular, two reduced order model based control approaches were considered: reduce the model then design the control versus design the control then reduce the order. The control laws were designed to mitigate a transient disturbance and is based on the linear quadratic regulation

(LQR) or to mitigate a persistent exogenous disturbance and is based the frequency shaping technique. The test bed for these control laws is a cantilever beam to which two PZT patches are mounted in a symmetric opposing fashion. The sensing device to be used for observation is a proximity probe. We chose to demonstrate the ideas in the context of a thin beam but the extension of analogous control methodologies to more complex systems is rather straight forward.

REFERENCES

- [1] H. T. Banks, S. C. Beeler, G. M. Kepler, and H. T. Tran, "Reduced order modeling and control of thin film growth in an HPCVD reactor," *SIAM J. Applied Mathematics*, vol. 62, no. 4, pp. 1251–1280, 2002.
- [2] H. V. Ly and H. T. Tran, "Proper orthogonal decomposition for flow calculation and optimal control in a horizontal CVD reactor," *Quarterly of Applied Mathematics*, vol. 60, no. 4, pp. 631–656, 2002.
- [3] H. T. Banks, G. M. Kepler, and H. T. Tran, "Compensator control for chemical vapor deposition film growth using reduced order design models," *IEEE Trans. on Semiconductor Manufacturing*, vol. 14, no. 3, pp. 231–241, 2001.
- [4] W. R. Graham, J. Peraire, and K. Y. Tang, "Optimal control of vortex shedding using low order models. Part I: Open-loop model development," *Int. J. for Numerical Methods and Engineering*, vol. 44, no. 7, pp. 945–972, 1999.
- [5] —, "Optimal control of vortex shedding using low order models. Part II: Model-based control," *Int. J. for Numerical Methods and Engineering*, vol. 44, no. 7, pp. 973–990, 1999.
- [6] S. S. Ravindran, "Adaptive reduced order controllers for a thermal flow system using proper orthogonal decomposition," *SIAM J. on Scientific Computing*, vol. 23, no. 6, pp. 1925–1943, 2002.
- [7] A. Atwell, J. T. Borggaard, and B. B. King, "Reduced order controllers for Burgers' equation with a nonlinear observer," *Int. J. of Applied Mathematics and Computational Science*, vol. 11, no. 6, pp. 1311–1330, 2001.
- [8] J. A. Atwell, "Proper orthogonal decomposition for reduced order control of partial differential equations," Ph.D. dissertation, Virginia Polytechnic Institute and State University, Blacksburg, Virginia, 2000.
- [9] J. A. Burns and B. B. King, "On the design of feedback controllers for a convecting fluid flow via reduced order modeling," in *Proceedings of the 1999 IEEE Int. Conf. on Control Applications*, Hawaii, 1999, pp. 1157–1162.
- [10] K. Fujimoto and J. M. Scherpen, "Balanced realization and model order reduction for nonlinear systems based on singular value analysis," *SIAM J. on Control and Optimization*, vol. 48, no. 7, pp. 4591–4623, 2010.
- [11] P. Odenacker and E. A. Jonckheere, "LQG balancing and reduced lqg compensation of symmetric passive systems," *Int. J. of Control*, vol. 41, no. 1, pp. 73–109, 1985.
- [12] E. A. Jonckheere and L. M. Silverman, "A new set of invariants for linear systems - Application to reduced order compensator design," *IEEE Trans. on Automatic Control*, vol. 28, pp. 953–964, 1983.
- [13] H. T. Banks, R. Smith, and Y. Wang, *Smart Material Structures: Modeling, Estimation, and Control*. Paris, France/Chichester, Great Britain: Masson/John Wiley and Sons, 1996.
- [14] B. M. Lewis, "Optimal control and shape design: Theory and applications," Ph.D. dissertation, North Carolina State University, Raleigh, North Carolina, 2003.
- [15] R. del Rosario, H. T. Tran, and H. T. Banks, "Proper orthogonal decomposition based control of transverse beam vibration: Experimental implementation," *IEEE Trans. on Control Systems Technol.*, vol. 10, pp. 717–726, 2002.
- [16] B. M. Lewis and H. T. Tran, "Real-time implementation of a frequency shaping controller on a cantilever beam," *Applied Numerical Mathematics*, vol. 57, pp. 778–790, 2007.
- [17] N. K. Gupta, "Frequency-shaped cost functionals: Extension of linear-quadratic-Gaussian design methods," *J. Guidance Control*, vol. 3, no. 6, pp. 529–535, 1980.
- [18] V. Sima and P. Benner, "Solving linear matrix equations with SLI-COT," in *Proceedings of the European Control Conference*, Cambridge, United Kingdom, 2003.
- [19] K. A. Camp and B. B. King, "A comparison of balanced truncation techniques for reduced order controllers," in *Proceedings of the 15th Int. Symposium on the Mathematical Theory of Networks and Systems*, Notre Dame, Indiana, 2001.
- [20] W. Gawronski, *Dynamics and Control of Structures: A Modal Approach*. New York, New York: Springer-Verlag, 1998.